

See discussions, stats, and author profiles for this publication at: <https://www.researchgate.net/publication/13679532>

# Calculated electrostatic gradients in recombinant human H-chain ferritin

ARTICLE *in* PROTEIN SCIENCE · MAY 1998

Impact Factor: 2.85 · DOI: 10.1002/pro.5560070502 · Source: PubMed

---

CITATIONS

85

---

READS

17

## 2 AUTHORS:



Trevor Douglas  
Indiana University Bloomington  
230 PUBLICATIONS 9,753 CITATIONS

[SEE PROFILE](#)



Daniel R Ripoll  
Biotechnology High Performance Computin...  
116 PUBLICATIONS 4,261 CITATIONS

[SEE PROFILE](#)

# Calculated electrostatic gradients in recombinant human H-chain ferritin

TREVOR DOUGLAS<sup>1</sup> AND DANIEL R. RIPOLL<sup>2</sup>

<sup>1</sup>Department of Chemistry, Temple University, Philadelphia, Pennsylvania 19122

<sup>2</sup>Cornell Theory Center, Cornell University, Ithaca, New York 14853

(RECEIVED November 24, 1997; ACCEPTED January 27, 1998)

## Abstract

Calculations to determine the electrostatic potential of the iron storage protein ferritin, using the human H-chain homopolymer (HuHF), reveal novel aspects of the protein. Some of the charge density correlates well with regions previously identified as active sites in the protein. The three-fold channels, the putative ferroxidase sites, and the nucleation sites all show expectedly negative values of the electrostatic potential. However, the outer entrance to the three-fold channels are surrounded by regions of positive potential, creating an electrostatic field directed toward the interior cavity. This electrostatic gradient provides a guidance mechanism for cations entering the protein cavity, indicating the three-fold channel as the major entrance to the protein.

Pathways from the three-fold channels, indicated by electrostatic gradients on the inner surface, lead to the ferroxidase center, the nucleation center and to the interior entrance to the four-fold channel. Six glutamic acid residues at the nucleation site give rise to a region of very negative potential, surrounding a small positively charged center due to the presence of two conserved arginine residues, R63, in close proximity (4.9 Å), suggesting that electrostatic fields could also play a role in the nucleation process.

A large gradient in the electrostatic potential at the 4-fold channel gives rise to a field directed outward from the internal cavity, indicating the possibility that this channel functions to expel cations from inside the protein. The 4-fold channel could therefore provide an exit pathway for protons during mineralization, or iron leaving the protein cavity during de-mineralization.

**Keywords:** electrostatic gradients; ferritin; iron; proton channel

Iron is an essential element for life. Due to its abundance and chemical versatility this element is found in many enzymes with a variety of functions (Crichton, 1991). However, iron is toxic and its concentration is under tight metabolic control. The iron storage protein, ferritin, functions to reversibly store iron as a particle of hydrated iron oxide (which may also contain phosphate) precipitated within the protein micelle, which renders it soluble yet unreactive (Mann et al., 1989). While the *in vivo* reaction of this protein is highly specific, yielding only the mineral ferrihydrite, synthetic reaction conditions can be altered to induce the formation of other minerals (Meldrum et al., 1991; Douglas, 1996 and references therein).

The three-dimensional structures of ferritin molecules from a number of different species have been determined (Lawson et al., 1991; Trikha et al., 1994, 1995; Michaux et al., 1996). These proteins have remarkably similar conformation and quaternary structures (Hempstead et al., 1997) even though some differ widely in primary sequence. A single ferritin molecule comprises 24 struc-

turally equivalent polypeptide subunits related by 4-fold, 3-fold, and 2-fold symmetry axes with one polypeptide chain per asymmetric unit. Mammalian ferritins contain a mixture of two different, but highly homologous, polypeptide subunit chains known as H (heavy) and L (light), present in variable proportions. Each subunit folds into a 4-helix bundle composed of two antiparallel helical pairs. The 24 subunits self-assemble to form a spherical molecule that defines an internal cavity roughly 8 nm in diameter. Channels of two types, along 3-fold and 4-fold symmetry axes, connect the inner cavity with the outside. Measurements of these channels from X-ray crystal structures show them to be roughly equal in size (ca. 3 Å diameter), but having quite different electrostatic characteristics.

The iron oxyhydroxide mineral ferrihydrite is formed and stored within the protein cavity. The mineralization mechanism is thought to involve both catalytic oxidation of a ferrous ion as well as controlled nucleation of the ferric-oxyhydroxide mineral. Ferroxidase centers implicated in the ferrous ion oxidation are only present on H chain subunits, in mammalian proteins, and are absent from L chain subunits (Lawson et al., 1991). However, L-chain subunits of human ferritin have been modified so as to impart ferroxidase activity (Levi et al., 1994).

Reprint requests to: Daniel R. Ripoll, Cornell Theory Center, Cornell University, 621 Frank Rhodes Building, Ithaca, New York 14853; e-mail: ripoll@tc.cornell.edu.

In the H-chain subunits of human ferritin, the ferroxidase site is comprised of a cluster of residues E27, Y34, E62, H65, E107, and Q141 arranged so as to bind a  $\mu$ -oxo Fe dimer (Treffry et al., 1997). By contrast in the L-chain subunits some of these residues are replaced (E27Y, E62K, H65G) giving rise to a salt bridge (Lawson et al., 1991), inactivating the ferroxidase activity, but having enhanced stability. In the structurally related bullfrog H-chain ferritin a ferric-tyrosinate complex has been suggested as an early precursor to core formation (Waldo et al., 1993) but which might alternatively contribute to the structure of the ferroxidase site (Treffry et al., 1995).

A putative nucleation site has been associated with the residues E61, E64, and E67 on the internal surface of the protein cavity, present in both L and H chain subunits of the mammalian proteins (Lawson et al., 1991). Additionally, residues E57 and E60 on L-chain subunits have been shown to play a key role in iron oxide nucleation (Santambrogio et al., 1996). However, not all of these residues are absolutely essential for core formation which will occur in the absence of either the ferroxidase site or the nucleation site but not in proteins where both sites have been altered (Wade et al., 1991). In mammalian systems, the variation in subunit proportions (H:L) is suggested to reflect different protein function. Proteins high in H subunit, having the ferroxidase center, might be important in Fe metabolism (Trikha et al., 1995), exhibiting efficient ferrous oxidation but forming a more disordered mineral which might be more easily mobilized. Ferritins high in L subunit show greater stability due to the introduction of the intersubunit salt bridge but also nucleate the iron oxide more effectively to form ordered mineral cores consistent with a storage function.

Investigations into the uptake and transport of Fe(II) across the protein shell of HuHF have focused on the 3-fold channel (Treffry et al., 1993; Levi et al., 1996). There is evidence that this funnel-shaped opening through the protein is the preferred and major pathway for Fe(II) uptake in most ferritin systems (Yablonski & Theil, 1992; Treffry et al., 1993). The channel is lined with at least six negatively charged residues (E134, D131 from each subunit), which are highly conserved among ferritins isolated from different sources. In addition, binding of metal ions has been shown to occur at the 3-fold channel of unmodified ferritins (Wardeska et al., 1986). It has also been demonstrated by X-ray analysis that metal binding is absent from 3-fold channels of mutant proteins where negatively charged residues are replaced by neutral ones (mutants E134A, or D131H-E134H) (Treffry et al., 1989, 1993).

Experiments with a series of 3-fold channel mutants of HuHF (E134A, D131H-E134H, D131A-E134A, D131I-E134F) revealed decreased rates of Fe(II) oxidation (Treffry et al., 1993; Levi et al., 1996). The substitutions D131A-E134A had less of an effect on core formation than the D131H-E134H substitutions. However, these rates were still significantly greater than either the ferroxidase mutants (E27A, E107A) or horse spleen L-chain ferritin (HoLFn), both of which have intact 3-fold channels but disrupted (or absent) ferroxidase centers (Treffry et al., 1993).

The fact that ferritin processes the highly positive ferric and ferrous ions suggests that electrostatic interactions could play an important role in the mechanism of iron mineralization. In general, electrostatic factors appear to play a dominant role in a wide variety of biominerization reactions (Mann et al., 1993).

Classical electrostatics, combined with very fast numerical algorithms and computational methods (Warwicker & Watson, 1982; Russell & Warshel, 1985; Klapper et al., 1986; Zauhar & Morgan, 1988; Davis & McCammon, 1990; Nicholls & Honig, 1991; Vorob-

jev et al., 1992) have been shown to be powerful tools for understanding a significant number of experimental findings in structural biology, biochemistry, and chemistry (Getzoff et al., 1983; Sines et al., 1990; Loewenthal et al., 1993; Ripoll et al., 1993; Gilson et al., 1994; Antosiewicz et al., 1995). Among other applications (see review by Honig & Nicholls, 1995), these theoretical approaches have been used successfully to design mutations in proteins with enhanced activity (Getzoff et al., 1992). There is continued interest in the detailed mechanism by which ferritin takes up, oxidizes, and mineralizes iron. Since our understanding of the structural basis of iron storage is incomplete, we have carried out a series of electrostatic calculations and in keeping with previous investigations (Harrison & Arosio, 1996 and references therein) we have used human H chain ferritin (HuHF) as a model, aimed at furthering our understanding of this important system.

## Results and discussion

### *Electrostatic potential on the outer surface*

The outside surface potential of the HuHF protein shows very pronounced electrostatic features. Overall negative potential values, attractive to cations, are dominant at the external surface of the molecule (Fig. 1). However, localized concentrations of positively charged residues give rise to regions of positive electrostatic potential of some significance.

### *Negative regions on the outer surface*

The outer molecular surface of HuHF exhibits well defined regions of negative potential where cations could interact strongly with the protein. These potential zones of interaction (Fig. 1) form a rhombic shape on the protein surface, where the vertices alternate between 3-fold and 4-fold channels ( $\sim 60 \text{ \AA}$  apart) and the edges are formed by two positive patches described in the next section. The negative potential in this region is mainly due to the residues D84, D89, D91, D92, and E94. A portion of the polypeptide segment containing these residues (residues 84 to 86) forms a two-stranded anti-parallel  $\beta$ -sheet together with the equivalent portion in a 2-fold symmetry-related subunit. Residues on these two strands give rise to a long fringe of highly negative values of the potential that connects two neighboring 4-fold channels and divides the negative rhombic patch into two halves. From this central negatively charged fringe, two secondary fringes branch out and connect with the region surrounding the 3-fold channel. Close to the 3-fold entrance, they merge and become very narrow ending on H118 and T122 at the 3-fold channel entrance. Surprisingly, a large number of asparagine and glutamine residues (N109, Q10, N11, Q112, N125), instead of aspartates and glutamates, line these low potential zones in the region proximal to the 3-fold entrance.

The negative fringe ( $80 \text{ \AA}$  in length) connecting neighboring 4-fold channels covers the external surface of ferritin right above two 2-fold symmetry-related ferroxidase sites. The region of the outer surface on top of each ferroxidase site forms a shallow basin as can be seen in Figure 1. It has been proposed (Lawson et al., 1991) that Fe(II) ions could reach the ferroxidase site by diffusion through a small nearby channel formed by helix A (residues 14 to 40) and helix C (residues 95 to 125) of a monomeric unit. Rapid uptake of iron ions could occur by relaxation of the interface between the helices. The very low potential values observed on the

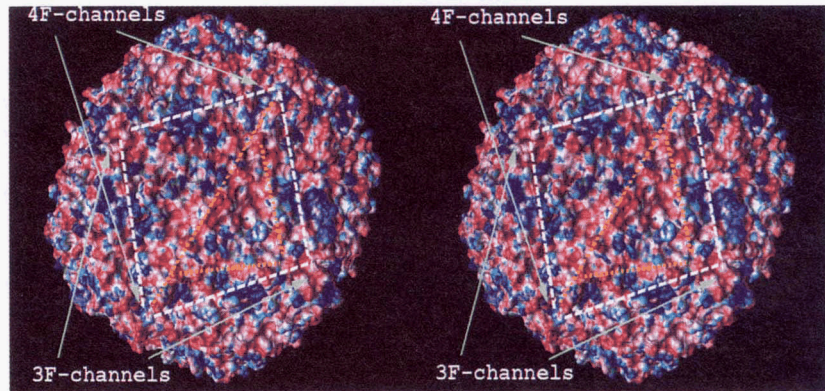


**Fig. 1.** Stereo image of the external surface of ferritin colored according to the values of the electrostatic potential. The dashed segments in white, connecting neighboring 3-fold and 4-fold channels, are used to define a rhombic area on the surface of the molecule. The electrostatic pattern in this rhombic area is repeated eight times over the entire molecular surface. The dashed segments in yellow are used to indicate three fringes of negative potential values over the ferritin surface. The following color convention is used to represent the values of the electrostatic potential,  $\Phi$  (in  $k_B T/e$  units), to the following scale:  $\Phi > +1$ , blue;  $+1 > \Phi > 0$  light blue;  $0 > \Phi > -1$ , white;  $-1 > \Phi > -4$ , light pink;  $-4 > \Phi > -6$ , darker pink;  $-6 > \Phi$ , red.

outer surface on top of each ferroxidase site are quite consistent with this hypothesis.

The outer region lining the entrance to the 3-fold channel has very negative potential values which extend across the protein shell to the interior of the central cavity. Major contributors to the negative potential at the outer entrance are the residues D123, D131, and E134. These negatively charged residues have been key to defining the role played by the 3-fold channel in iron transport across the protein shell (Treffry et al., 1993; Harrison & Arosio, 1996), in mammalian ferritin systems.

#### Positive regions on the outer surface

Our calculations show that the negative outer entrance to the 3-fold channel, mentioned previously, is conspicuously surrounded by three regions of positive potential values (Fig. 2A). Each region lies halfway ( $\sim 30$  Å) between the 3-fold and the nearest 4-fold channel. As can be seen in Figure 2B, these regions of positive potential, adjacent to the negative opening of the 3-fold channel, give rise to an electrostatic field that should direct cations strongly toward the channel entrance. In this way the inherent funnel shape of the 3-fold channel is substantially widened, in addition to being extended well beyond the protein surface. The probability of a noncharged particle entering the ferritin cavity simply through collisions is rather small. A rough estimate of this probability can be obtained by representing the ferritin molecule as a sphere of 60 Å radius, and by assuming that this type of particle is able to penetrate only through the eight 3-fold channels (the approximate cross-sectional area of each channel entrance is  $25 \text{ } \text{\AA}^2$ ). In this case, the probability that a particle would enter the cavity after a single collision, computed as a ratio between the sum of the areas of the eight 3-fold channel entrances to the whole ferritin surface, is 1.8%. On the other hand, if the particle is positively charged, it will be directed toward the cavity by the electrostatic field "funnel" described above. Assuming that the area of attraction of this "funnel" is defined by a triangular cross-sectional area with vertices at the centers of three positive patches that surround each 3-fold channel ( $\sim 625 \text{ } \text{\AA}^2$ ), then the probability of a cation colliding with the ferritin molecule and entering the cavity is estimated

as 44%. Thus, the positive patches on the outer surface of ferritin appear to be involved in an electrostatic guidance mechanism, similar to that observed previously with other enzymes (Getzoff et al., 1983; Ripoll et al., 1993). It appears the cooperative effect of the negatively charged residues previously mentioned together with the positively charged residues create an electrostatic gradient, which is difficult to completely disrupt by alterations to only the negative regions of the 3-fold channel. Thus, the mutants D131H-E134H and D131A-E134A show only slightly diminished rates of Fe(II) oxidation, but the mutations do not completely eliminate Fe(II) uptake (Treffry et al., 1993).

The regions of positive potential described above originate from a high density of positively charged residues, the most important contributors being the highly conserved residues R9, R43, R79, and K108, and the less conserved ones K119 and K174. (Not all residues belong to the same monomeric unit.) It is interesting to note that the guanidinium groups of two arginines from different subunits (R43 and R79) are arranged very close together (the distance between NH1 (R43) to NH2 (R79) is 4.0 Å). This close packing of positively charged groups should, in principle, lead to a strong electrostatic repulsion. However, this type of interaction is usually mediated by water molecules.

The 4-fold channel has been regarded as largely hydrophobic due to the presence of 12 leucine residues (3 from each subunit) which line the channel, although this is mitigated somewhat in HuHF by the presence of four histidine residues (Harrison & Arosio, 1996). The 4-fold channel appears narrower than the 3-fold channel. Our calculations show that the potential on the exterior of this channel tend to be positive, as can be seen from Figure 3. Major contributors to this positive region are the four symmetrical N-termini of the  $\alpha$ -helices formed by residues L173 to G184, and residues R156 and K157 (conserved). Clearly the external surface in the region of the 4-fold channel is repulsive to positively charged ions.

Another interesting feature of this region are four symmetric E162 residues which protrude significantly from the molecular surface of the protein and stand as pillars to the outer opening of the 4-fold channel. This gives the 4-fold channel a significantly different electrostatic topology from the 3-fold channel.

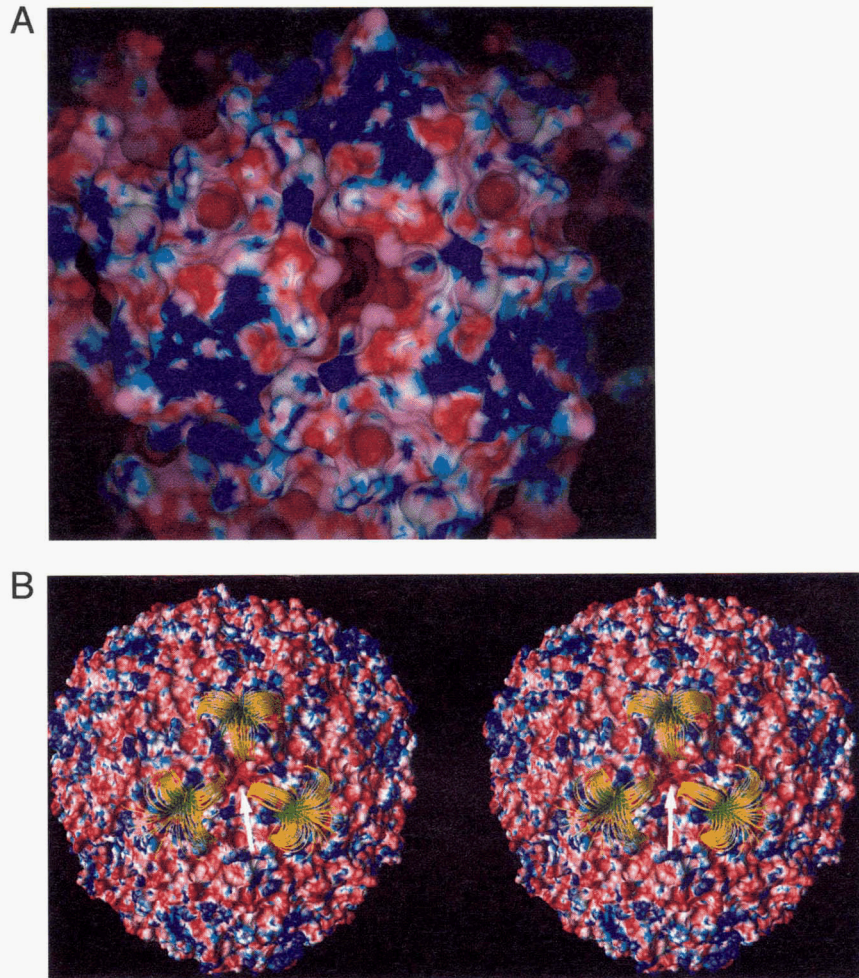


**Fig. 2.** **A:** View of a 3-fold-channel region on the external surface of ferritin. The surface has been colored according to the values of the electrostatic potential (see Fig. 1 for a description of the color convention). **B:** Stereo view of the ferritin molecular surface colored according to the values of the electrostatic potential. A white arrow indicates the entrance to the 3-fold channel. In addition, a set of electrostatic field lines initiated from points near the molecular surface show the "funnel" shape of the electrostatic field.

#### *Electrostatic potential and field inside the cavity*

The potential on the interior surface of the ferritin shell is, like the outer surface, mostly negative with only a few regions with positive values. Four main areas of negative potential were observed on the internal surface. These are: (1) the region around the 3-fold channel, (2) the ferroxidase site region, (3) the nucleation site region, and (4) the region around the internal entrance to the 4-fold channel. Viewing the cavity toward one of the 3-fold channels (as shown in Fig. 4) illustrates this distribution of charge.

#### *The 3-fold channel regions*

The internal entrance to the 3-fold channel has the lowest negative values of the potential anywhere inside the protein. As mentioned previously, this negative patch extends along the wide channel running across the protein shell from the outside to the inside. Residues in the interior of the cavity contributing to the negative potential in this region are: E131 and D134 from three different subunits forming the wall of the channel and the three symmetric

E140 residues which line the interior entrance of the channel. This region is surrounded by a group of lysine residues (K68, K71, R76, K143, and K146). Fe(II) ions entering the protein (presumably as  $(Fe(OH)_{aq})^+$ ) via the 3-fold channel would encounter these positive residues as an electrostatic wall with the only pathway indicated by E140 directing positive ions toward the ferroxidase center. This corroborates a previous suggestion that a roughly 20 Å pathway exists for the movement of ferrous ions from the 3-fold channel to the ferroxidase site (Treffry et al., 1993). The presence of such a strong electrostatic field at the interior entrance to the 3-fold channel, apparently directing cations into the cavity raises questions about the possible pathway(s) for cations leaving the interior cavity (see later), since ferritin is implicated as an iron buffer controlling both the sequestration and release of iron.

Another interesting aspect to the distribution of positively charged residues is the location of the highly conserved residues K68, R76, and K146, as well as the less conserved K71 and K143. These residues are positioned in the internal wall of the cavity immediately below the residues which generate the large positive potential patch on the external surface. In other words, the internal and

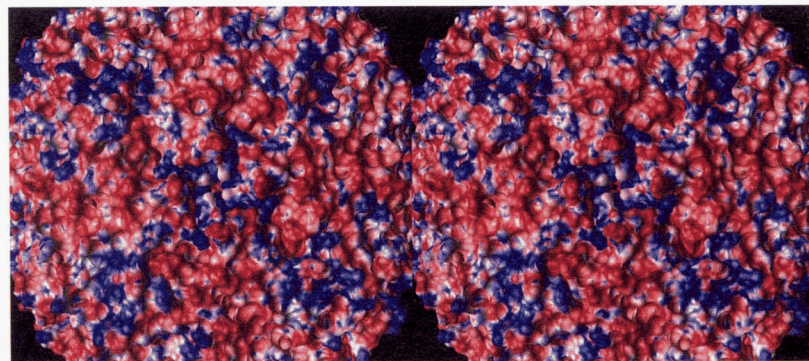


**Fig. 3.** A stereo view of the region surrounding a 4-fold channel on the external surface of ferritin. The surface has been colored according to the values of the electrostatic potential (see Fig. 1 for a description of the color convention).

external regions having the largest positive potential values are actually connected through the molecular wall. In addition, many of these residues are highly conserved among ferritins, which might indicate the importance of this region of the molecule. Experimental work to elucidate its role is clearly needed.

#### The ferroxidase site

The ferroxidase site too has very negative values of the potential which can be attributed to residues E27, E61, E62, E107, E140, and E147 in the region of the ferroxidase site. This is consistent with what is known about specific Fe(II) binding to these residues although it indicates that the electrostatic effect at this site extends beyond the residues responsible for metal binding (E27, Y34, E62, H65, E107, and Q141) to include neighboring residues that contribute to the overall electrostatic of the site making it highly

attractive to incoming ferrous ions. The electrostatic gradient between the 3-fold channel and the ferroxidase site merely directs cations toward the ferroxidase site, but it is the specific binding at this site that appears crucial for catalytic oxidation. Thus, the specificity of the ferroxidase site goes beyond electrostatics. This is illustrated by experiments, in horse spleen ferritin, which have shown that while Fe(II) is catalytically oxidized, the electrostatically similar Mn(II) is not catalytically oxidized at the ferroxidase site (Meldrum et al., 1995).

#### The nucleation site

The arrangement of charges at the nucleation site of HuHF is remarkable (Fig. 5). The nucleation site occurs at the interface between two subunit monomers where the residues form a small pocket. Six glutamic acid residues (E61, E64 and, E67 from each

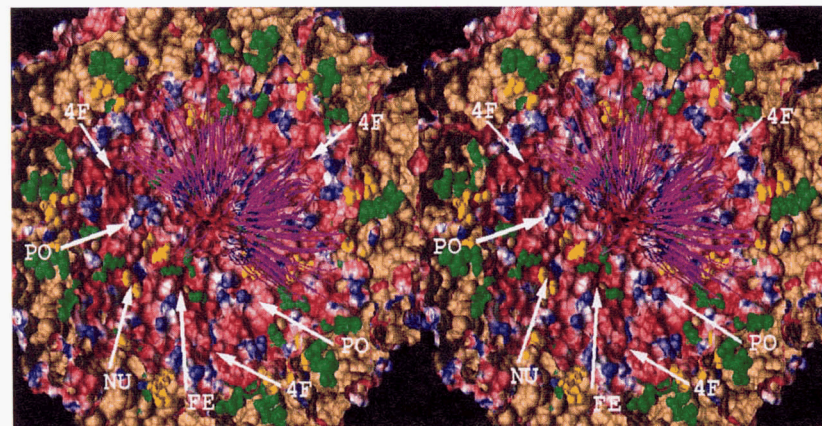


**Fig. 4.** Stereo view of the interior surface of ferritin colored according to the values of the electrostatic potential. The molecular surface of ferritin was cut in half by an imaginary plane. A portion of the molecular surface exposed to the center of the cavity (interior surface) is shown with the 3-fold channel (not labeled) positioned at the center of the figure. The internal sides (the ones facing toward the protein core) of both interior and exterior surfaces are shown in gold. The glutamic acid residues associated with the ferroxidase center (FE) are shown in green, while the glutamic acid residues associated with the nucleation center (NU) are colored yellow. The position of the ferroxidase (FE) and the nucleation (NU) centers, as well as the 4-fold channel (4F) and the groups of positively charged residues (PO) are indicated by the white arrows. A set of electrostatic field lines, initiated from a semi-spherical grid, are also shown. For visual purposes, the position of the grid was chosen in such a manner that almost all the field lines terminate on the right side of the internal surface. The direction of the electrostatic field is indicated by the blue-to-magenta direction on the lines (see Fig. 1 for a description of the color convention).

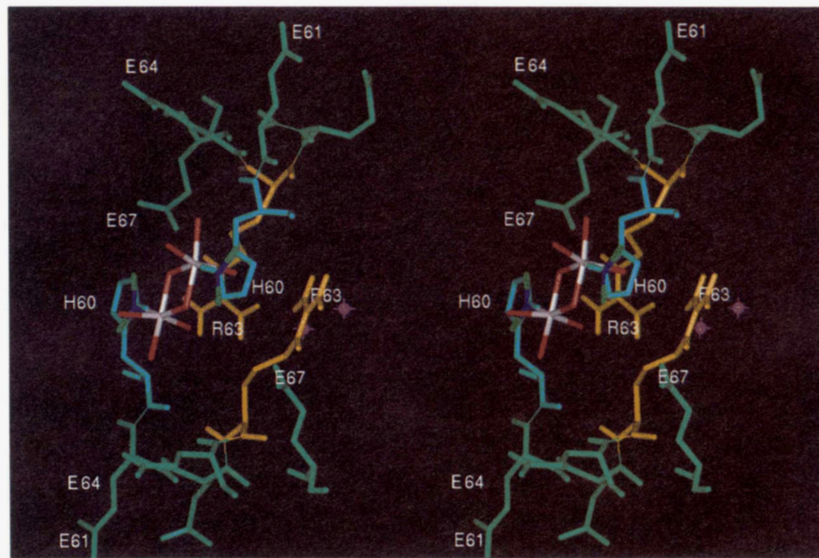


**Fig. 5.** Stereo view of the residues forming one of the nucleation sites in ferritin with a dinuclear iron(III) compound bound to it. The iron(III)  $\mu$ -oxo dimer position is a result of a computer docking experiment. The positions of some of the ferritin residues are different from the ones given in the crystallographic data (Lawson et al., 1991), e.g., the side chain positions of H60 residues were modified slightly to show that these residues could be involved in binding the iron(III) dimer. However, two O atoms corresponding to experimentally-observed water molecules are shown (in magenta) in their crystallographic positions. The figure was generated using InsightII (Molecular Simulations Inc., USA).

of the two different monomeric units) form a ring of negative charges. Each nucleation site is linked with two oxidation sites where the E61 residues appear to lie at the interface between nucleation and oxidation sites. A large number of electric field lines in the interior of the cavity are directed toward the nucleation site, as shown in Figure 4, indicating that this region is very attractive to positively-charged ions. Two buried arginines (R63 from the 2-fold related monomers), at the center of that pocket, generate a small positive region in the center of that ring. The nucleation site is therefore characterized by high charge density, although in a far more complex arrangement than previously predicted (Mann et al., 1989). Mutant proteins in which the glutamic acid residues have been replaced by alanine residues show diminished rates of mineralization (Wade et al., 1991). This mutation deletes the electrostatic driving force for ferric ion aggregation (nucleation) while leaving a region that retains substantial positive charge, repulsive to ferric ions within the protein cavity.

The side chains of the two highly conserved R63 residues (Harrison & Arosio, 1996) at the center of the nucleation site are arranged in an unusual conformation. They run antiparallel to each other, as shown in Figure 5, with the NH<sub>1</sub> atoms from the two different guanidinium groups separated by 4.9 Å, and almost buried behind two H60 residues. Two water molecules are trapped between the arginines and the internal wall of the cavity, which mediate the otherwise repulsive interactions between the positively charged groups. These residues have been implicated in porphyrin binding to ferritin (Michaux et al., 1996). Since the presence of a positively charged residue at position 63 in the sequence is highly conserved, it is possible that the R63 residues are involved in the nucleation process. One possibility is that these groups participate in the nucleation process by stabilizing a ferric hexqua-like species, a precursor to the inorganic polymerization forming the oxy-

hydroxide mineral. To check the feasibility of such a mechanism, we carried out a simple docking experiment. Figure 5 shows the result of this simulation where a dinuclear iron(III) compound was “docked” at the center of the nucleation site. The geometrical parameters for the ferric  $\mu$ -oxo dimer were obtained from a similar model compound (Powell et al., 1995). Since the compound used to derive our model has nitrogen atoms bound to each iron(III), our docking model assumed that the N atoms from the two H60 residues at the nucleation site can bind to the iron(III) dimer in a similar manner. The side chains of the H60 residues were slightly altered from the crystallographic positions to show that the residues could perfectly bind to the iron(III) atoms in the dimer. Two oxygen atoms (from water molecules) bound to each of the iron(III) atoms are positioned on top to the guanidinium groups of the R63 residues and in close proximity. This type of interaction mimics the interaction of the R63 residues with two oxygen atoms from crystallographic waters (shown in magenta) under the guanidinium groups. Furthermore, the iron dimer is in reasonable position to start the process of crystal growth toward the center of the cavity. As a consequence, this relatively trivial docking experiment shows that residues in the nucleation site are able to satisfy geometrical as well as simple energetic considerations in a model that could provide a view of the nucleation process. Interestingly, the docking experiments suggest that the H60 actually stabilizes this  $\mu$ -oxo dimer, which might result in an inhibition of the hydrolysis polymerization. Interestingly, this is consistent with a recent observation that human L-chain ferritin HuLF (having residues E60, E57) exhibits enhanced ability to nucleate iron oxide, relative to either HuHF or mutant HuLF (H57E, H60E) (Santambrogio et al., 1996). It is possible that H60 in HuHF can stabilize the Fe  $\mu$ -oxo dimer thereby limiting hydrolysis. The role of H57/E57 is currently being explored.

### Internal entrance to the 4-fold channel

The electrostatic potential at the internal region surrounding the 4-fold channel was also observed to be very negative, with values similar to those in the oxidation and nucleation site regions. This is shown in Figure 4 by the large number of field lines directed toward this region. The potential values in this particular region can be ascribed to the carboxyl groups ( $\text{COO}^-$ ) at the C-terminal ends of the four monomers forming the channel and the free carbonyl ( $\text{C=O}$ ) groups at the C-termini of four  $\alpha$ -helices involving residues L165 to G176. It is worth noting that the residues forming these four  $\alpha$ -helical segments define almost entirely the walls of the 4-fold channel. The  $\alpha$ -helices run parallel to each other with their C-termini pointing inward (toward the center of the cavity). The internal border of the 4-fold channel, lined by the side chains of four H173 residues, is relatively small when compared to the corresponding external border of the same channel or the borders at the 3-fold channels (it can be circumscribed to a square with a side of 3.22 Å and the N atom of each H173 residues on each vertices). Mutant HuHF proteins lacking the last 22 amino acids at the carboxyl terminus (Levi et al., 1988) assemble in a similar manner as native HuHF and the ferroxidase activity is conserved. However, these mutants are unable to form a stable iron oxide core, which suggests that the integrity of the 4-fold channel is an important element for core formation.

Surprisingly, our calculations show that there is an abrupt change in the electrostatic potential when entering into the 4-fold channel, i.e., the hydrophobic groups seem to amplify the effects of residues R156, K157, K172, and the free amino ( $\text{NH}$ ) groups at the N-termini of the four  $\alpha$ -helices (L165–G176), leading to positive values of the potential inside the channel and at the region that extend to the outer surface, already described. This remarkable feature, not previously observed, creates an electrostatic field which is directed out from the cavity inside the 4-fold channel (Fig. 6). From an

electrostatic point of view, the following picture emerges from the previous analysis: free positively charged ions ( $\text{H}^+$ , Fe(II)) upon reduction of the ferrihydrite core) accumulating within the cavity may reach the 4-fold channel region directed by the local electrostatic field. Any positive ion that is allowed to enter a 4-fold channel by the gatekeeper H173 residues will feel an electrostatic gradient pushing it across the protein shell to the outside.

Although the 4-fold channel is lined with eight leucine residues and four histidines, the observed gradient across the protein shell is in contrast to its presumed apolar character (Harrison & Arosio, 1996). This electrostatic gradient, however, indicates a new and plausible function for the 4-fold channel in ferritin, as a backdoor through which ions, specifically protons, might pass. As shown in Figure 6, the gradient field lines from the inside terminate at the residues E162, on the outside of the protein, indicating those as potential terminal proton acceptors in the translocation of protons across the protein shell.

The electrostatic properties of the 4-fold channel, described above, are not expected to be significantly different in ferritin assemblies from different subunit composition, since a comparison of difference sequences (Harrison & Arosio, 1996) indicates that the residue E162 and the presence of positively charged residues at positions 157 and 172 are highly conserved. A calculation of the electrostatic gradient at this site using the modification E162Q revealed an almost identical field gradient.

Proton transfer is a central issue in the mineralization reaction of iron oxides and we speculate that the function of the 4-fold channel might be to remove protons from the site of mineralization. The dehydration polymerization of the ferric ion to form an oxyhydroxide mineral such as ferrihydrite generates up to 4 protons per iron (Xu & Chasteen, 1991). Since polymorph selection in iron oxyhydroxides is highly pH dependent (Schwertmann & Cornell, 1991), it follows that efficient proton removal from the site of mineralization is critical to maintain the integrity of the mineral

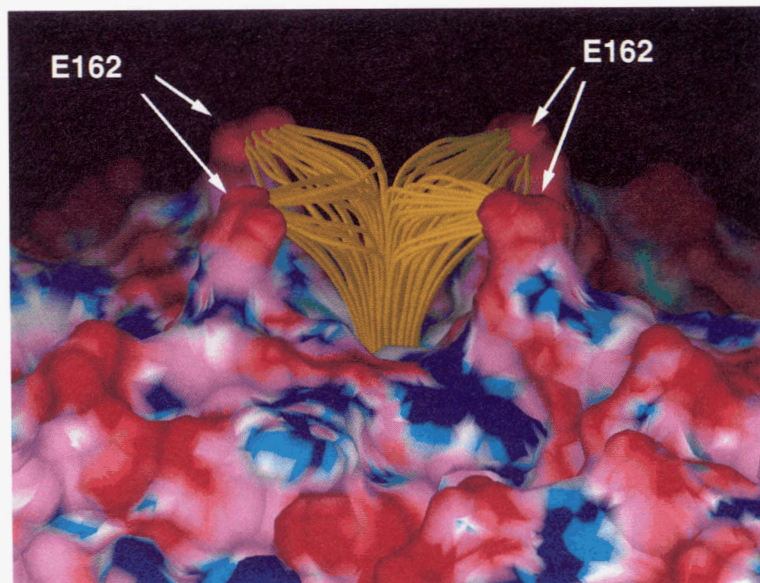


**Fig. 6.** Side view of the external opening of a 4-fold channel colored according to the electrostatic potential. A set of electrostatic field lines are shown to indicate that the electrostatic field inside this channel is directed outward. The lines were initiated from points at a small grid ( $4 \text{ \AA} \times 4 \text{ \AA}$ ; not shown) located inside the 4-fold channel. Note also that these field lines terminate at the carboxyl groups of the four residues E162 (see Fig. 1 for a description of the color convention).

phase. Under physiological conditions ferritin mineralizes only the mineral ferrihydrite (native and reconstituted proteins). However, in the absence of apoferritin, under these conditions, bulk precipitation of lepidocrocite occurs (Ford et al., 1984). The formation of ferrihydrite, a kinetically stabilized mineral phase, is consistent with an efficient removal of protons from the site of mineralization within the protein, a proton shuttle. As the mineralization reaction proceeds and local pH drops due to H<sup>+</sup> formation, it is conceivable that a cooperative proton transfer (or conduction) moves protons from the nucleation site to the outside of the protein via the 4-fold channel. The movement of protons could be greatly facilitated by this large electrostatic field.

### Summary

Our results indicate a high degree of electrostatic interaction and cooperativity between subunits. These calculations, combined with powerful graphic tools, allow us to focus attention on certain regions of this large and complex system, identifying important residues previously uninvestigated. It is clear that cooperative effects in structure and charge lead to the presence of electrostatic gradients, which are significant to the overall functioning of the protein.

The presence of regions of positive potential surrounding the entrance to the negative 3-fold channel enhances the effective size of the channel and may function as a funnel to direct cations such as Fe(II) through this channel to the interior of the protein. In addition, there is a clear electrostatic pathway from the interior entrance of the 3-fold channel directly to the ferroxidase site.

The electrostatic fields also lead to an apparent streaming of cations toward the nucleation site, a region a large negative potential. Two conserved arginine residues (R63) at the center of the nucleation site seem to be associated with a possible electrostatic function in the mineralization process at the nucleation site. Selective stabilization of a ferric  $\mu$ -oxo dimer at the nucleation site might explain differences in crystal nucleation efficiencies between H- and L-chain subunits.

In addition, the somewhat surprising presence of a large electrostatic gradient through the 4-fold channel, previously thought to be apolar, suggests the possibility that this channel might function as a pathway for the removal of protons from within the protein cavity. Proton removal is a key step in the mechanism of the ferrihydrite mineral formation. The recombinant human H ferritin provides an excellent model for these calculations because of its extensive structural and kinetic characterization. However, experiments and theoretical simulations are underway to explore other physiologically important heteropolymers of mixed L- and H-chain ferritins, now that crystallographic data for both chains are available.

### Materials and methods

The all-atom model of ferritin was built from the data available (Protein Data Bank) for the recombinant human H chain mutant, engineered for enhanced crystallization (Lawson et al., 1991). In this protein K86 is replaced by Q86. This mutation alters intermolecular interactions to facilitate crystallization but has no observable effect on iron uptake (Treffry et al., 1993). The program SYBYL (Tripos, Inc., USA) was used to add the unobserved atoms and polar hydrogens to the ferritin monomer, and to generate the three-dimensional coordinates for each of the 24 monomers in the quaternary structure. Following this initial procedure, we carried out a series of electrostatic calculations on the modeled structure

using the program DelPhi (B. Honig, pers. comm.; Klapper et al., 1986; Gilson et al., 1987; Gilson & Honig, 1987, 1988; Nicholls & Honig, 1991). This program solves the Poisson-Boltzmann equation numerically using a finite-difference algorithm. The ferritin molecule was assumed to be immersed in an aqueous solution, containing counterions (ionic strength of 0.10 M).

The Debye-Hückel model was used to represent the environment surrounding the protein. The solvent and the protein molecule were treated as homogeneous dielectric media: water was described as a high-dielectric medium,  $\epsilon_{\text{solv}} = 80.0$  and the protein itself was approximated by a cavity of low dielectric constant  $\epsilon_{\text{prot}} = 4.0$ . Finally, heavy atoms and polar hydrogens were assigned point charges in accord with the united-atom approximation used in the AMBER program (Singh et al., 1986; Weiner et al., 1986). The whole system (protein plus solvent) was included in a cubic grid of 129 × 129 × 129 nodes.

An initial DelPhi calculation was carried out with the protein cavity occupying 30% of the grid volume. Data from this first calculation were subsequently used to define the boundary conditions of a second run in which the protein was occupying approximately 90% of the grid volume (distance between grid points of 1.03 Å). For this purpose, the focusing feature available within DelPhi was used. Visualization of the electrostatic properties was carried out using the IBM Visualization Data Explorer DX (IBM Corporation, USA), and a set of chemistry applications (Gillilan & Ripoll, 1995). Construction of the molecular surfaces of the protein was accomplished using the program SURF (Varshney & Brooks, 1993). Graphics manipulation, analysis of the ferritin structure, and manual docking experiment were carried out using the InsightII software (Molecular Simulations Inc., USA)

The following color convention is used to represent the values of the electrostatic potential,  $\Phi$  (in  $k_B T/e$  units; with  $k_B$  the Boltzmann constant, e the electronic charge unit, and T temperature), to the following scale:  $\Phi > +1$ , blue;  $+1 > \Phi > 0$  light blue;  $0 > \Phi > -1$ , white;  $-1 > \Phi > -4$ , light pink;  $-4 > \Phi > -6$ , darker pink;  $-6 > \Phi$ , red.

Special computer requirements were needed to carry out the visualization part of this research. A wide node of an IBM-SP2 with 1GB of memory was used to run the program DX.

### Acknowledgments

We are grateful to C.H. Faerman for helpful suggestions and discussions. We thank B. Honig (Columbia University) for a copy of the program DelPhi and R. Gillilan for his chemistry modules for the program Data Explorer (IBM Corp.). The simulations in this work were carried out at the Cornell Theory Center which is funded in part by the National Science Foundation, New York State, the IBM Corporation, and members of its Corporate Research Institute. This research was supported by a grant from the National Institutes of Health (P41RR-04293). Acknowledgment is made to the Donors of The Petroleum Research Fund, administered by the American Chemical Society, for partial support of this research (TD).

### References

- Antosiewicz J, McCammon JA, Wlodek ST, Gilson MK. 1995. Simulation of charge-mutant acetylcholinesterases. *Biochemistry* 34:4211–4219.
- Crichton RR. 1991. *Inorganic biochemistry of iron metabolism*. Chichester: Ellis Horwood.
- Davis ME, McCammon JA. 1990. Electrostatics in biomolecular structure and dynamics. *Chem Rev* 90:509–521.
- Douglas T. 1996. Biomimetic synthesis of nanoscale particles in organized protein cages. In: Mann S, ed. *Biomimetic approaches in materials science*. New York: VCH Publishers. pp 91–115.

- Ford GC, Harrison PM, Rice DW, Smith JMA, Treffry A, White JL, Yariv J. 1984. Ferritin: Design and formation of an iron-storage molecule. *Philos Trans R Soc London Ser B* 304:551–565.
- Getzoff ED, Cabelli DE, Fisher CL, Parge HE, Viezzoli MS, Banci L, Hallewell RA. 1992. Faster superoxide dismutase mutants designed by enhancing electrostatic guidance. *Nature* 358:347–351.
- Getzoff ED, Tainer JA, Weiner PK, Kollman PA, Richardson JS, Richardson DC. 1983. Electrostatic recognition between superoxide and copper, zinc superoxide dismutase. *Nature* 306:287–290.
- Gillilan RE, Ripoll DR. 1995. Visualizing enzyme electrostatics with IBM Visualization Data Explorer. In: Bowie JE, ed. *Data visualization in molecular science*. Menlo Park, CA: Manning Publications Co. and Addison-Wesley Publishing Company Inc. pp 61–81.
- Gilson MK, Honig BH. 1987. Calculation of electrostatic potential in an enzyme active site. *Nature* 330:84–86.
- Gilson MK, Honig BH. 1988. Energetic of charge-charge interactions in proteins. *Proteins Struct Funct Genet* 3:32–52.
- Gilson MK, Sharp KA, Honig BH. 1987. Calculating electrostatic interactions in bio-molecules: Method and error assessment. *J Comput Chem* 9:327–335.
- Gilson MK, Straatsma TP, McCammon JA, Ripoll DR, Faerman CH, Silman I, Sussman JL. 1994. Open “back door” in a molecular dynamics simulation of acetylcholinesterase. *Science* 263:1276–1278.
- Harrison PM, Arosio P. 1996. The ferritins: Molecular properties, iron storage function and cellular regulation. *Biochim Biophys Acta* 1275:161–203.
- Hempstead PD, Yewdall SJ, Fernie AR, Lawson DM, Artymuik PJ, Rice DW, Ford GC, Harrison PM. 1997. Comparison of the three-dimensional structures of recombinant human H and horse L ferritins at high resolution. *J Mol Biol* 268:424–448.
- Honig B, Nicholls A. 1995. Classical electrostatics in biology and chemistry. *Science* 268:1144–1149.
- Klapper I, Hagstrom R, Fine RM, Sharp KA, Gilson MK, Honig B. 1986. Focusing of electric fields in the active site of Cu-Zn superoxide dismutase: Effects of ionic strength and amino-acid modification. *Proteins Struct Funct Genet* 1:47–59.
- Lawson DM, Artymuik PJ, Yewdall SJ, Smith JMA, Livingstone JC, Treffry A, Luzzago A, Levi S, Arosio P, Cesareni G, Thomas CD, Shaw WV, Harrison PM. 1991. Solving the structure of human H ferritin by genetically engineering intermolecular crystal contacts. *Nature* 349:541–544.
- Levi S, Corsi B, Rovida E, Cozzi A, Santambrogio P, Albertini A, Arosio P. 1994. Construction of a ferroxidase center in human ferritin L-chain. *J Biol Chem* 269:30334–30339.
- Levi S, Luzzago A, Cesareni G, Cozzi A, Francheschinelli F, Albertini A, Arosio P. 1988. Mechanism of ferritin iron uptake: Activity of the H-chain and deletion mapping of the ferro-oxidase site. *J Biol Chem* 263:18086–18092.
- Levi S, Santambrogio P, Corsi B, Cozzi A, Arosio P. 1996. Evidence that residues exposed on the three-fold channels have active roles in the mechanism of ferritin iron incorporation. *Biochem J* 317:467–473.
- Loewenthal R, Sancho J, Reinikainen T, Fersht AJ. 1993. Long-range surface charge-charge interactions in proteins. Comparison of experimental results with calculations from a theoretical method. *J Mol Biol* 232:574–583.
- Mann S, Archibald DD, Didymus JM, Douglas T, Heywood BR, Meldrum FC, Reeves NJ. 1993. Crystallization at inorganic-organic interfaces: Biomaterials and biomimetic synthesis. *Science* 261:1286–1292.
- Mann S, Webb J, Williams RJP, eds. 1989. *Biomineralization: Chemical and biochemical perspectives*. New York: VCH.
- Meldrum FC, Douglas T, Levi S, Arosio P, Mann S. 1995. Reconstitution of manganese oxide cores in horse spleen and recombinant ferritins. *J Inorg Biochem* 58:59–68.
- Meldrum FC, Wade VI, Nimmo DL, Heywood BR, Mann S. 1991. Synthesis of inorganic nanophase materials in supramolecular protein cages. *Nature* 349:684–687.
- Michaux MA, Dautant A, Gallois B, Granier T, d'Estaintot BL, Precigoux G. 1996. Structural investigation of the complexation properties between horse spleen apoferritin and metalloporphyrins. *Proteins* 24:314–321.
- Nicholls A, Honig B. 1991. A rapid finite difference algorithm, utilizing successive over-relaxation to solve the Poisson-Boltzmann equation. *J Comp Chem* 12:435–445.
- Powell AK, Heath SL, Gatteschi D, Pardi L, Sessoli R, Spina G, Del Giallo F, Pieralli F. 1995. Synthesis, structure, and magnetic properties of  $\text{Fe}_2$ ,  $\text{Fe}_{17}$ , and  $\text{Fe}_{19}$  oxo-bridged iron clusters: The stabilization of high ground state spins by cluster aggregates. *J Am Chem Soc* 117:2491–2502.
- Ripoll DR, Faerman CH, Axelsen PH, Silman I, Sussman JL. 1993. An electrostatic mechanism for substrate guidance down the aromatic gorge of acetylcholinesterase. *Proc Natl Acad Sci USA* 90:5128–5132.
- Russell ST, Warshel A. 1985. Calculations of electrostatic energies in proteins. The energetics of ionized groups in bovine pancreatic trypsin inhibitor. *J Mol Biol* 185:389–404.
- Santambrogio P, Levi S, Cozzi A, Corsi B, Arosio P. 1996. Evidence that the specificity of iron incorporation into homopolymers of human L- and H-chains is conferred by the nucleation and ferroxidase centers. *Biochem J* 314:139–144.
- Schwertmann U, Cornell RM. 1991. *Iron oxides in the laboratory; preparation and characterization*. Weinheim: VCH.
- Sines JJ, Allison SA, McCammon JA. 1990. Point charge distributions and electrostatic steering in enzymes/substrate encounter: Brownian dynamics of modified copper/zinc superoxide dismutases. *Biochemistry* 29:9403–9412.
- Singh UC, Weiner PK, Caldwell J, Kollman PA. 1986. *AMBER. Version 3.0*. San Francisco, CA: University of California.
- Treffry A, Bauminger ER, Hechel D, Hodson NW, Nowik I, Yewdall SJ, Harrison PM. 1993. Defining the roles of the threefold channels in iron uptake, iron oxidation and iron-core formation in ferritin: a study aided by site-directed mutagenesis. *Biochem J* 296:721–728.
- Treffry A, Harrison PM, Luzzago A, Cesareni G. 1989. Recombinant H-chain ferritins: Effects of changes in the 3-fold channels. *FEBS Lett* 247:268–272.
- Treffry A, Zhao Z, Quail MA, Guest JR, Harrison PM. 1995. Iron(II) oxidation by H chain ferritin: Evidence from site-directed mutagenesis that a transient blue species is formed at the dinuclear iron center. *Biochemistry* 34:15204–15213.
- Treffry A, Zhao Z, Quail MA, Guest JR, Harrison PM. 1997. Dinuclear center of ferritin: Studies of iron binding and oxidation show differences in the two iron sites. *Biochemistry* 36:432–441.
- Trikha J, Theil EC, Allewell NM. 1995. High resolution crystal structures of amphibian red-cell L ferritin: Potential roles for structural plasticity and solvation in function. *J Mol Biol* 248:949–967.
- Trikha J, Waldo GS, Lewandowski FA, Ha Y, Theil EC, Weber PC, Allewell NM. 1994. Crystallization and structural analysis of bullfrog red cell L-subunit ferritins. *Proteins* 18:107–118.
- Varshney A, Brooks FP Jr. 1993. Fast analytical computation for Richards's smooth molecular surface. In: Nielson GM, Bergeron D, eds. *IEEE Visualization '93*. San Jose, CA: IEEE. p 300.
- Vorobjev YN, Grant JA, Scheraga HA. 1992. A combined iterative and boundary element approach for solution of the nonlinear Poisson-Boltzmann equation. *J Am Chem Soc* 114:3189–3196.
- Wade VI, Levi S, Arosio P, Treffry A, Harrison PM, Mann S. 1991. Influence of site-directed modifications on the formation of iron cores in ferritin. *J Mol Biol* 221:1443–1452.
- Waldo GS, Ling J, Sanders-Loehr J, Theil EC. 1993. Formation of an Fe(II)-tyrosinate complex during biomineratization of H-subunit ferritin. *Science* 259:796–798.
- Wardeska JG, Viglione B, Chasteen ND. 1986. Metal ion complexes of apoferitin. *J Biol Chem* 261:6677–6683.
- Warwicker J, Watson HC. 1982. Calculation of electric potential in the active site cleft due to  $\alpha$ -helix dipoles. *J Mol Biol* 157:671–679.
- Weiner SJ, Kollman PA, Nguyen DT, Case DA. 1986. An all atom force field for simulations of proteins and nucleic acids. *J Comp Chem* 7:230–252.
- Xu B, Chasteen ND. 1991. Iron oxidation chemistry in ferritin. *J Biol Chem* 266:19965–19970.
- Yablonski MJ, Theil EC. 1992. A possible role for the conserved trimer interface of ferritin in iron incorporation. *Biochemistry* 31:9680–9684.
- Zauhar RJ, Morgan RS. 1988. The rigorous computation of the molecular electric potential. *J Comp Chem* 9:171–187.